

Interannual variability of the zonal sea surface slope in the equatorial Atlantic during the 1990s

C. Provost ^{*}, N. Chouaib, A. Spadone, L. Bunge, S. Arnault, E. Sultan

*LODYC UMR7617 CNRS/IRD/IUPMCI/MNHN, Université P. et M. Curie, 4 place Jussieu, Tour 45-5ème étage,
Case 100, 75252 Paris Cedex 05, France*

Received 27 October 2004; received in revised form 1 June 2005; accepted 4 June 2005

Abstract

Altimetry data have proven themselves essential for the early detection, analysis and monitoring of large scale tropical anomalies associated with El Niño in the Pacific. Warm events in the Atlantic are much weaker than in the Pacific and are partially masked by the strong seasonal cycle. Satellite altimetric data permits one to estimate the zonal sea surface slope variations at the equator in the Atlantic with sufficient accuracy for resolving interannual sea surface slope variations. The altimetry-derived slope is here shown to detect Atlantic warm events. For all warm events, anomalies in sea surface slope tend to lead SST. In the mid-1990s, the equatorial interannual variability is dominated by 17-month period events which exhibit the structure observed in local coupled ocean–atmosphere warm events (zonal wind stress weakening and zonal surface slope relaxation, warm SST, excess precipitation). The frequency of occurrence of these Atlantic warm events is seen to have increased during the mid-1990s.

© 2005 COSPAR. Published by Elsevier Ltd. All rights reserved.

Keywords: Altimetry; Ocean circulation; Equatorial dynamics; Climate variability

1. Introduction

The tropical Atlantic is dominated by a strong annual cycle forced by the seasonally varying trade winds. Katz et al. (1986), using in situ data collected during the 2-year long FOCAL/SEQUAL experiment, showed that the zonal slope of the thermocline varies almost exactly in phase with the winds, in agreement with Sverdup's (1947) linear theory. The thermocline is relatively horizontal during the first half of the year when the winds along the equator are weak, and it has a westward steep slope when the westward winds intensify during the second half of the year. Besides the seasonal cycle, variations were also seen between the first and second year of the FOCAL/SEQUAL experiment.

Satellite altimetry has been used recently to examine the large-scale and low-frequency variability of the surface currents in the tropical Atlantic (Arnault and Kestenare, 2004). For the equatorial Atlantic, Provost et al. (2004) showed that the zonal sea surface slope anomaly can be computed from satellite altimetry with an accuracy of about 1 mm/deg and that the slope anomaly time series formed using data from the TOPEX/Poséidon satellite can be accurately continued with data from the newer Jason satellite. Following this validation study, we investigate here the interannual variability of the altimeter-derived sea surface slope anomaly at the equator, and compare it with that of the surface winds, sea surface temperatures, and precipitation.

2. Data processing

TOPEX/Poséidon (hereafter T/P) and Jason geophysical data records (GDR) within the tropical Atlantic were

^{*} Corresponding author. Tel.: +33 144 273 481; fax: +33 144 277 159.

E-mail address: cp@lodyc.jussieu.fr (C. Provost).

processed as detailed in Arnault and Kestenare (2004). The zonal sea surface slope anomaly (SSSA) was then obtained as explained in Provost et al. (2004) (Fig. 1). Sensitivity studies in that paper demonstrated that the error bar on the SSSA is less than 1 mm/deg whereas the annual signal has an amplitude of about 10 mm/deg. The shift between T/P and Jason altimetric data occurs in August 2002, but no significant differences were observed between the two altimeters during the commissioning phase. Altogether, the altimetric data extends from October 1992 to March 2003, thus providing the first SSSA time series with that duration (Fig. 2).

We compared the zonal wind stress (τ_x) and sea surface temperature (SST) in the equatorial Atlantic from various sources. Differences are not significant for our analyses and we present here τ_x and SST from the operational model reanalyses ERA 40 of the European Centre for Medium-range Weather Forecasting (ECMWF). The model assimilates data and involves comprehensive use of both satellite and in situ data. We used the daily ERA 40 data to produce zonal wind stress and SST time series averaged over a 30W–10W longitudinal band and a latitudinal range of 1.69° on either side of the equator sampled at the same rate as the T/P and Jason satellites (every 9.9156 days precisely) shown in Fig. 2.

We also examined precipitation from the Global Precipitation Climatology Project (GPCP), which provides monthly mean precipitation data on a 2.5° by 2.5° latitude–longitude grid. A time series of precipitation was produced by averaging data from 40W to 10E along the equator and subsampling it at the altimetric time step (Fig. 2).

The precise choice of the box boundaries used in forming the time series does not influence significantly the results (see discussion section).

A continuous wavelet transform (CWT) with a complex-valued Morlet wavelet and amplitude normalization was used to estimate the time/frequency characteristics of the different components embedded in the time series and to compute spectra. The dominant components are extracted from the transform ridges, defined here as the locations of maximum transform modulus. For example, the annual and semi-annual components, which dominate the four time series, are shown in red and green on Fig. 2. The continuous cross wavelet transform was also used to estimate the instantaneous phase difference and instantaneous delay between series (see appendix of Jury et al., 2002 for a description of the method).

3. The seasonal cycle in SSSA, winds, SST and precipitation

The annual and semi-annual signals dominate the spectral decomposition of the four time series (SSSA, zonal wind stress, SST, and precipitation) (Fig. 3(a)).

The amplitude of the mean SSSA seasonal cycle is about 10 mm/deg with a minimum in August–September (when the absolute westward slope is maximum) and a maximum in May–June (when the absolute slope weakens). The slope standard deviation around the mean annual cycle is about 1 mm/deg and is roughly constant in time. The mean zonal wind stress at the

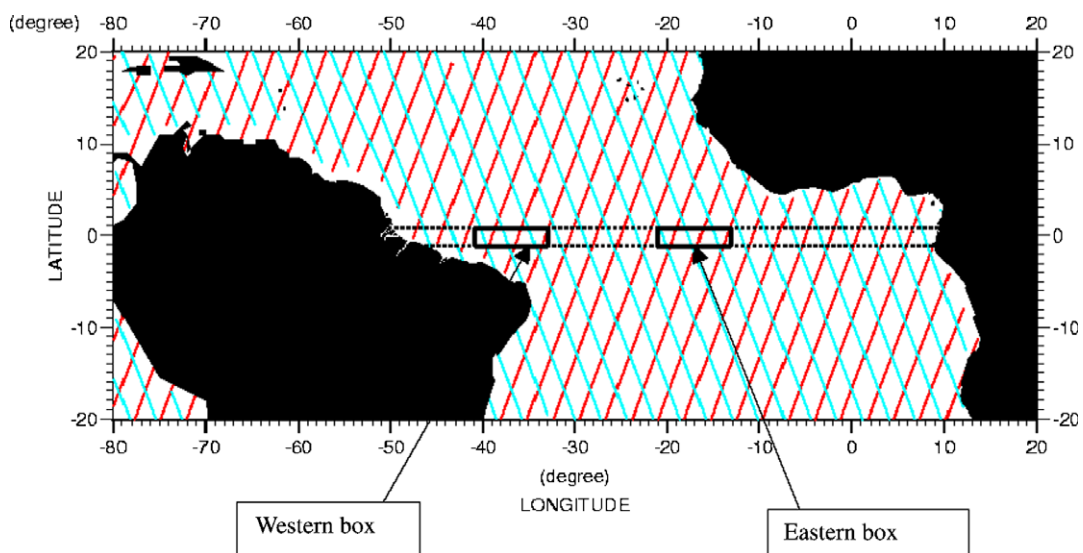


Fig. 1. T/P and Jason tracks over the tropical Atlantic. The sea level slope anomaly time series is computed as the time series difference between the mean values of the SLA over the western and eastern boxes divided by the distance between the box centers. The western and eastern boxes are straddling the equator with 2° latitudinal extension. Sensitivity of the calculation to the size and location of the box is discussed in Provost et al. (2004).

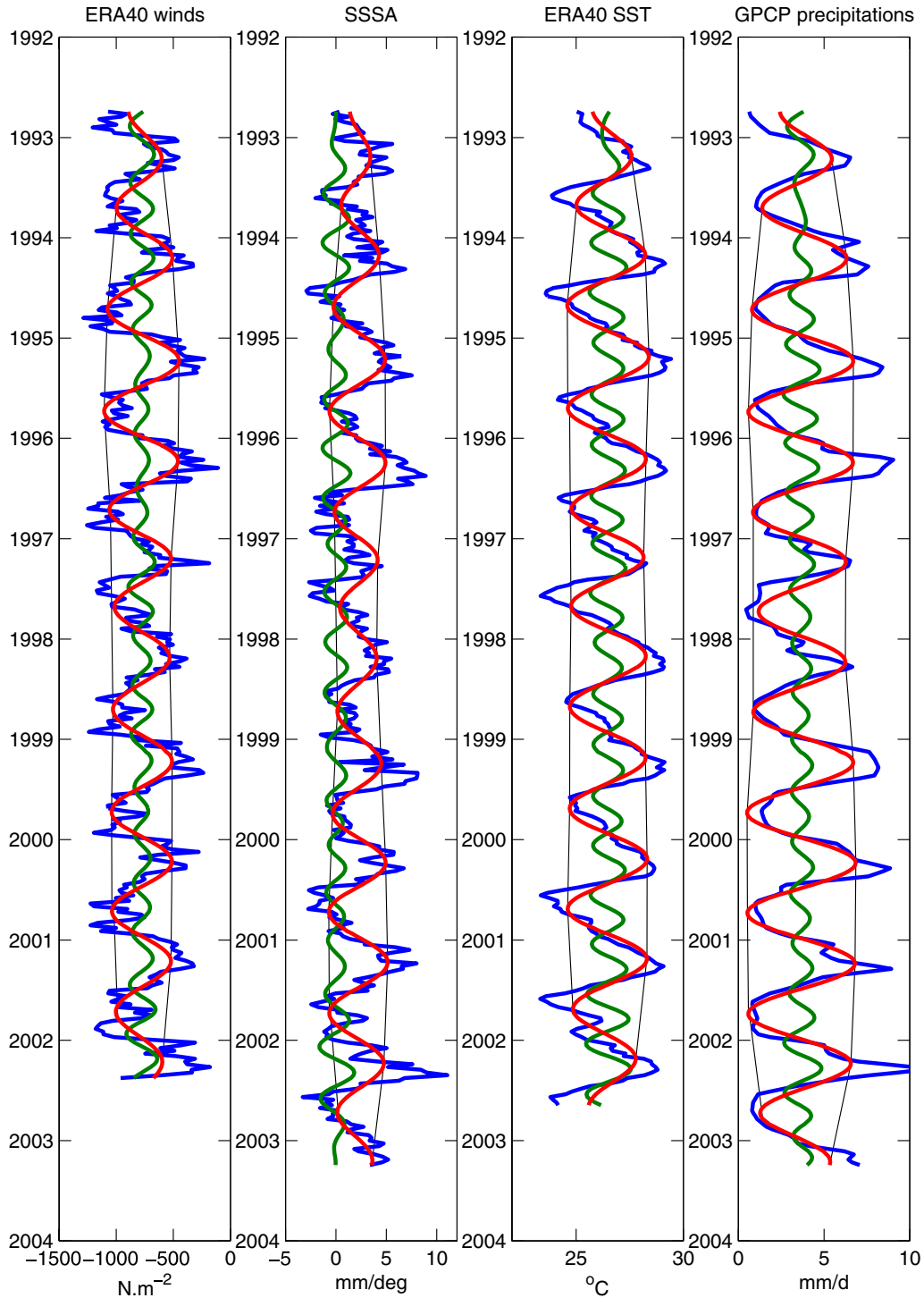


Fig. 2. Variables from left to right: Mean zonal wind stress (τ_x) over a region bounded by 30W, 10W, 1.8N and 1.8S from ECMWF ERA40 reanalyses. Units are N m^{-2} . Sea surface slope anomaly (SSSA) at the equator over 10 years estimated from T/P and Jason (end of the time series) in mm/deg. Mean sea surface temperature (SST) in $^{\circ}\text{C}$ over the same region as the zonal wind stress from ECMWF ERA40 reanalyses. Mean precipitation (P) in mm/day over the region bounded by 40W 10E and 2.5N 2.5S from Global Precipitation Climatology Project (GPCP). The annual (in red) and the semi-annual (green) components have been extracted from ridges of maximum amplitude of the continuous wavelet transform. In grey, the envelope of the maxima of the annual component. (For interpretation of the references to colour in this figure legend, the reader is referred to the Web version of this article.)

equator, to the west (negative) for the entire year, exhibits a strong seasonal cycle (peak-to-peak amplitude of 700 N m^{-2}) with a relaxation of the winds in

April and maximum intensities in November–December. Thus, the SSSA is maximum (i.e. the absolute westward slope minimum) when the winds are the

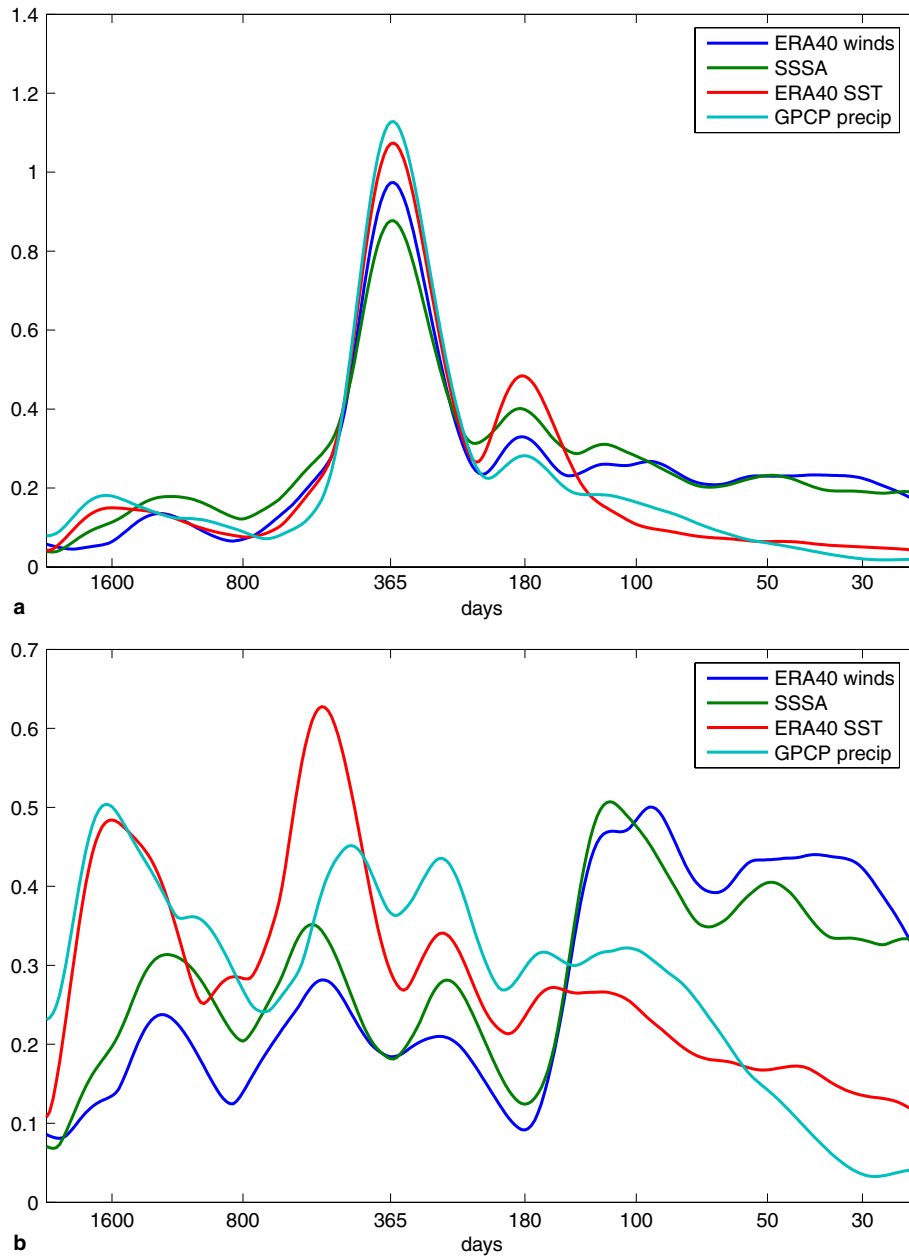


Fig. 3. (a) Normalized spectra of the SSSA (green), zonal wind stress (dark blue), SST (red) and precipitation (light blue) time series. The annual and semi-annual peaks dominate. (b) Normalized spectra of SSSA (green), zonal wind stress (dark blue), SST (red) and precipitation (light blue) time series after removal of the annual and semi-annual components and filtering out high frequencies (periods less than 100 days). Main peaks, in order of decreasing amplitude are at 15–17 month period (450–510 days), intra-seasonal time scales (~ 8 –9 months) and low frequencies (>3.5 years). (For interpretation of the references to colour in this figure legend, the reader is referred to the Web version of this article.)

weakest (March–May) in agreement with previous studies (e.g. Katz et al., 1986). On average the slope builds up rapidly in the three months from May to August, and slowly relaxes during the rest of the year to reach its minimum in May when the SSSA is maximum. Similarly, the seasonal warming and cooling phases of the SST are highly asymmetric in their durations with the cooling taking only three months (May through July) while the warming takes up three times longer; this feature has been previously observed and discussed by Okumura and Xie (2004).

The seasonal cycles of SSSA, zonal wind stress, SST and precipitation contain annual and semi-annual components (extracted as discussed in Section 2) which together explain 75%, 81%, 91% and 89% of the total variance of each field respectively, with the amplitude of the semi-annual component being between half and one-third that of the annual component (Fig. 2). Since precipitation data are monthly means, the percentage of variance explained above are computed with SSSA, zonal wind stress and SST data filtered at one month (Hanning filter over 3 points) for sake of homogeneity.

The annual components (in red) for SSSA, winds, SST and precipitation are all in phase with each other. The wind semi-annual component (green) leads the SSSA, SST, and precipitation semi-annual components by about a month. For the zonal wind stress time series, the extrema of the annual and semi-annual components coincide, and a local maximum in the autumn is due to the second peak of the semi-annual component. For the SSSA, SST and precipitation time series, the extrema of the annual and semi-annual components are separated from each other by lags of about two months. These lags lead to the observed asymmetry in the annual cycle described above, with a cooling phase being roughly one-third the duration of the warming phase.

These annual and semi-annual components exhibit low-frequency amplitude modulation. The time series are not long enough to accurately describe this low-frequency variability; however the hint at an approximately 5-year modulation time scale for the annual component is apparent.

4. Interannual variability

Subtracting the mean annual cycle and removing high frequency fluctuations with a Hanning filter over 10 time steps (100 days) produces residual time series with somewhat similar spectral content, with, in order of decreasing amounts, energy at 15–17 month period (450–510 days), intra-seasonal time scales (~ 8 –9 months) and low frequencies (>3.5 years) (Fig. 3(b)).

These residual time series are highly correlated (Fig. 4). The correlation coefficient is greater than 0.74 for wind and SSSA, greater than 0.75 for SSSA and SST, greater than 0.6 for SSSA and precipitation. Residual variations are of the same amplitude as the semi-annual component of the seasonal cycle (about 3 to 4 mm/deg for SSSA, 200 N m^{-2} for τ_x , 1°C for SST and 2 mm/day for precipitation). The mean lag between wind and SSSA is 13 days (wind leading) and SSSA leads SST by 17 days on average (this is discussed further below).

Six anomalous warm events characterized by high SST, low winds, high slope anomaly (i.e. relaxed sea surface slope) and excess precipitation can be identified between 1992 and 2002 (Fig. 3). The relative amplitudes of the anomalies vary from event to event. The more striking SSSA event occurs in 1996 (event 3) and is followed by a strong cold (La Niña) episode. This 1996–1997 event is prevalent, in terms of intensity in both SSSA and SST. The cold phase corresponds to the strongest winds. However, the wind relaxation associated with event 3 is equal in magnitude to that seen in events 2, 4 and 5 (1995, 1998 and 1999). Thus, similar wind relaxations do not produce the same variations in the slope or in SST. The timing of the wind anomaly within the annual cycle may seem to be a possible explanation, yet the

comparable wind relaxations for events 2 and 3 occurred both in May–June but lead to different amplitude anomalies. Pre-existing La Niña conditions may also limit the impact of the wind relaxation. For example, it seems that La Niña conditions, like those in 1997, tend to limit the impact of the subsequent wind relaxation anomaly (event 4). Therefore, although correlations are high, there is not a strict correspondence between the strength of events in both wind and SSSA.

The spatial structure of the interannual variability was examined through an EOF decomposition of the SST and wind stress fields in the equatorial band (3N–3S) (not shown). The first mode reveals a spatial structure similar to the one described by Tseng and Mechoso (2001), that is, a maximum warming at 10W and the equator, and anomalous convergence towards the warming center in winds; this pattern is strongly reminiscent of the equatorial modes of the coupled atmosphere–ocean system seen during a Pacific ENSO event. The time series associated with this mode is here found to have a spectral peak at about 17 months.

A mode of variability, similar to the Pacific ENSO, has been identified in the Tropical Atlantic Ocean (e.g., Philander, 1986; Zebiak, 1993; Carton and Huang, 1994) and is associated with enhanced precipitation along the equator (Ruiz-Barradas et al., 2000). Associated with the warming SSTs are changes in the overlying atmosphere. The equatorial winds relax and corresponding increases in diabatic heating in the mid-troposphere occur along with a southward shift in tropical convection (Carton et al., 1996). The autonomy and frequency of occurrence of Atlantic warm events have been subject of controversy. Based on a numerical study, Zebiak (1993) suggests that an equatorial coupled mode exists in the Atlantic, has a quasi-quadrannual period and is evanescent, this implies that external perturbations are required to maintain such Atlantic interannual variability. Handoh and Bigg (2000) analyzed the 1996–1997 event in SLA, SST, wind and out-going long wave radiation and showed distinct evidence for a purely internal and self-sustaining coupled atmosphere–ocean oscillation, which they call Equatorial Atlantic Oscillation (EAO). They also examined 18–35 month band pass-filtered global fields of SST and SLP extending from 1871 to 1994 and only identify 6 EAOs during those 120 years. Ruiz-Barradas et al. (2000) and Tseng and Mechoso (2001) analyzed winds and SST over the period 1964–1997 and observed an Atlantic ‘Niño’ mode with a 27.3-month occurrence period (quasi-biennial), therefore with a much higher frequency than found by Handoh and Bigg (2000). Tseng and Mechoso’s coupled modeling (2001) suggests that the quasi-biennial oscillation observed in the equatorial Atlantic is generated by local atmosphere–ocean interactions without systematic forcing from the variability outside that ocean basin. Similarly, the anomalous shifts in equatorial winds

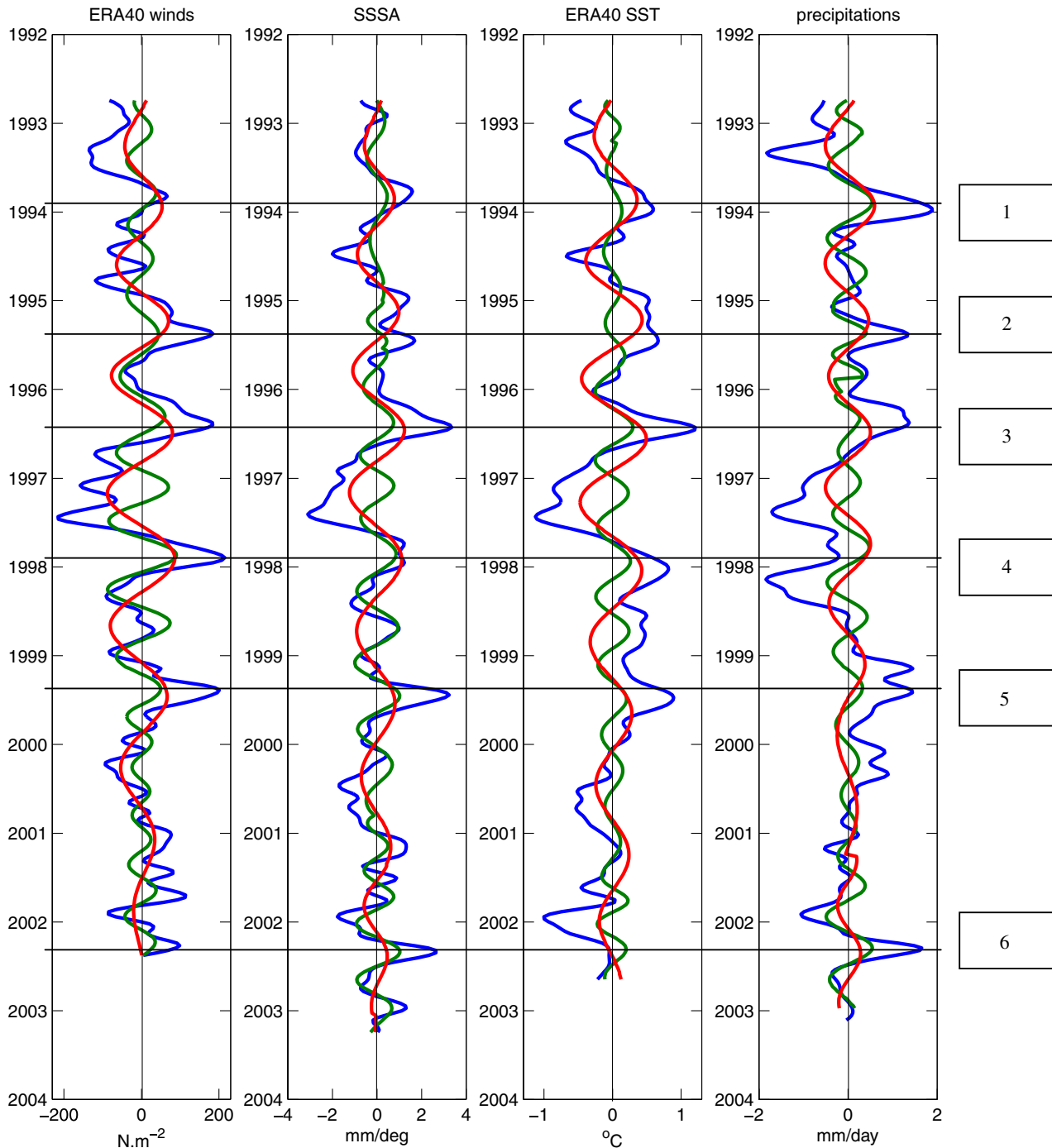


Fig. 4. SSSA, zonal wind stress, SST and precipitation anomaly times series after removing the seasonal cycle and filtering out fluctuations with periods below 100 days. Warm events are labeled from 1 to 6. Components at 17 months, 8 months are plotted, respectively, in red and green. (For interpretation of the references to colour in this figure legend, the reader is referred to the Web version of this article.)

and tropical convection associated with the Atlantic Niño are well captured by a number of Atlantic GCMs that are forced by Atlantic Niño SST anomalies (Chang et al., 2000; Sutton et al., 2000; Okumura and Xie, 2004), confirming that they result from air-sea interaction much like their El Niño counterparts in the Pacific.

The correspondence seen here between warm events and precipitation (Fig. 4) corroborates Ruiz-Barradas

et al. (2000) observations. Again, we notice that the warm event 4 following the strong 1997 La Niña conditions, although strong in winds only manages to bring precipitation from a low to a “normal” level and not to an excess precipitation.

Event 6 seems to be a singular event with respect to the other ones as it has no or little apparent signal in SST although it is characterized by high SSSA, high

precipitation and high winds (Fig. 4). Indeed the positive SST anomaly distribution along the equator for event 6 is quite different from that for the other events. The positive anomaly is confined to the east of 23W whereas a negative SST anomaly extends from the west to 23W. Therefore, the SST anomaly averaged over the box 30W–10W is small. For the other events, the positive SST anomaly extends from 30W to the Gulf of Guinea. The SSSA is high because the SLA is particularly low in the West. The precipitation anomaly is high all along the equator after a long period of anomalously low precipitation (Fig. 4).

For all warm events, although the details of the phase relationship vary, SSSA tend to lead SST (Fig. 4). This is similar to what is observed in the Pacific. In the Pacific, much of the early El Niño signal occurs below the ocean surface, in the form of Kelvin waves triggered by wind relaxation. Thus, altimetry can detect El Niño signals slightly before SST measurements can. This time difference is small, between two weeks and a month in the Pacific. Here, in Fig. 4, the lag between SSSA and SST is

variable: it appears somewhat larger for warm events 1 and 4 than for events 3 and 5. The mean lag between SSSA and SST is 17 days. A precise estimation of this lag requires further study, and, in particular an estimation of the SSSA with a higher temporal resolution than 10 days.

We checked for possible remote influences on our data time series. We concentrated on two major climatic indices: the Pacific El Niño Southern Oscillation (ENSO) and North Atlantic Oscillation (NAO) indices. We could not find coherent relationships between those indices and the warm events observed in the 1990s in the Atlantic.

The rate of occurrence of the warm events is obviously higher in the mid-1990s, about one every 17 months, than the 27 month repeat period described by Tseng and Mechoso (2001) or Ruiz-Barradas et al. (2000). The 10-year duration of the altimetric time series is too short for detecting possible variations in the rate of occurrence of the Atlantic warm events. To address this question, we analyze the whole SST time series from

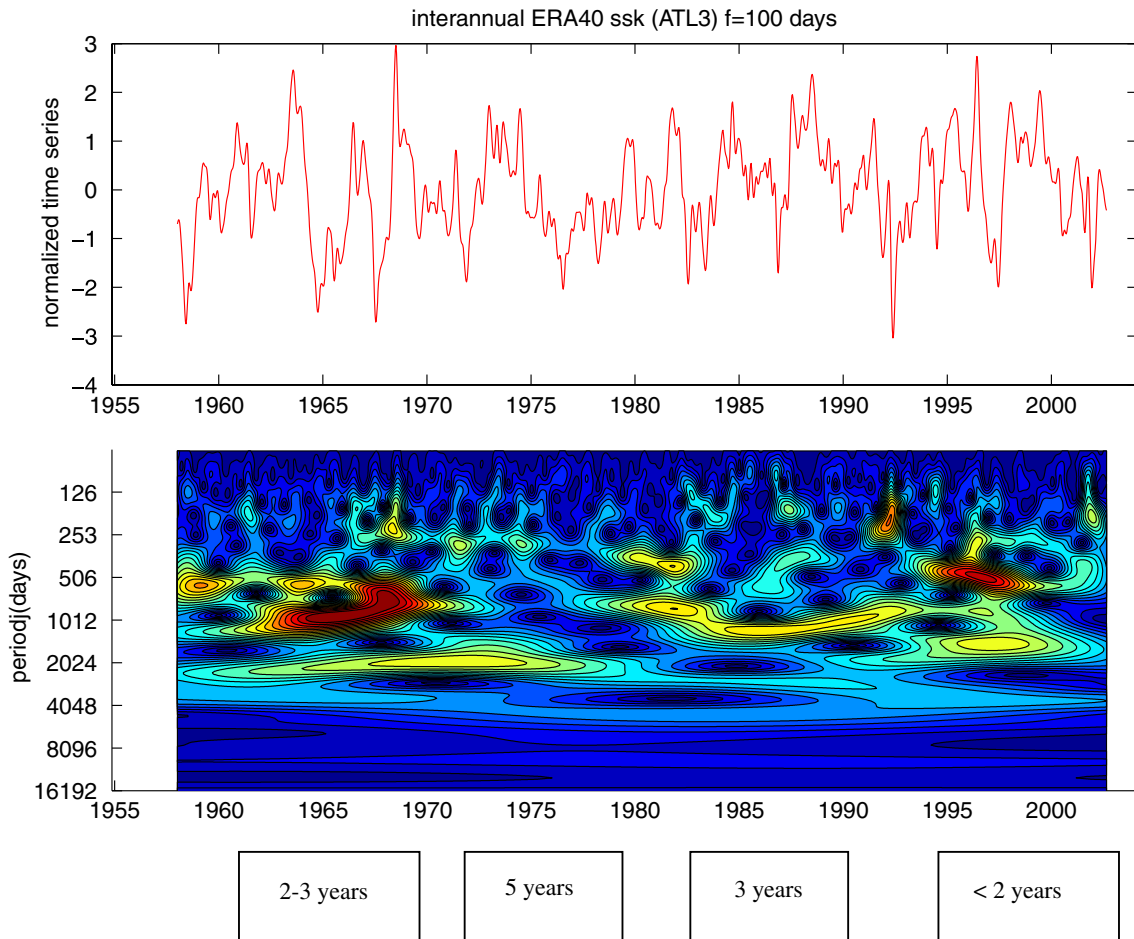


Fig. 5. Normalized mean SST over ATL3 box (20W–10W 3N–3S) from ERA40 starting in 1958 after removing the seasonal cycle and wavelet transform modulus: maximum energy is found at about 2–3 years in the 1960s, 5 years in the 1970s, 3 years in the 1980s and less than 2 years in the 1990s.

ERA 40 (1958–2002) using the CWT after removing the mean annual cycle (Fig. 5). Indeed, frequency of warm events has varied in the second half of the 20th century: frequency of 2 to 3 years in the 1960s, lower frequency greater than 5 years in the 1970s, about 3 years in the 1980s and less than 2 years in the 1990s. Decadal variations in intensity are also observed: warm events were strong in the 1960s, weak in the 1970s and 1980s, strong again the 1990s. Thus, the periodicity of the Atlantic Niño seems to vary considerably. The reasons for these changes are subject of investigations. Key parameters such as the heat content of the tropical thermocline have only recently come to be measured regularly, while theoretical attention seems to be focusing on changes in the rates of subduction within the tropical thermocline (Xie and Carton, 2004).

5. Summary

Atlantic warm events can be detected with satellite altimetry even though they are much weaker than those in the Pacific (sea level anomalies of a few cm compared to up to 30 cm). The zonal sea surface slope anomaly may be computed with an accuracy of about 1 mm/deg whereas its seasonal variation is on the order of 10 mm/deg with interannual variations of roughly 3–4 mm/deg.

The correlations between variations at interannual time scales of the zonal sea surface slope anomaly, zonal wind stress, SST and precipitation along the equator are remarkable. We performed sensitivity studies which showed that the high levels of correlation are robust and not sensitive to the precise choice of the boxes over which the parameters are averaged upon. The high correlation between the zonal sea surface slope and the zonal wind stress at the interannual time scale shows that the Sverdrup balance is extremely well satisfied quasi-synoptically. This balance is not of course the whole story. For example, the anomalous low winds of spring 1995 and winter 1997, as low as those of spring 1996 or summer 1999, did not produce a relaxation of the slope as large as the one of 1996 or 1999. Pre-existing La Niña-type conditions and extra-equatorial interannual modes of variability such as the dipole could certainly be expected to also have an influence.

SST anomalies associated to warm events tend to lag SSSA and zonal wind stress anomalies. As in the Pacific, warm events can be detected slightly earlier in the altimetry-derived slope than in SST. This result could be very useful for prediction purposes. A precise estimation of the lag between the signatures of warm events in altimetry and SST requires further study.

The 10 day resolution of the altimetric series produced here does not permit a precise evaluation of the

phase difference between the two time series. This should be possible soon with composited products produced using data from several altimetric satellite such as those at 3.5 day resolution provided by CLS-Argos since February 19, 2003.

EOFs describe a generic structure for Atlantic warm events (Tseng and Mechoso, 2001). However, Atlantic warm events exhibit significant differences in structure, duration and time of occurrence within the seasonal cycle from one another. To understand those differences, we have undertaken a precise examination of the zonal extent of the anomalies. Unfortunately, the gappy nature of the in situ data is a serious limitation to the description of the vertical structure of the anomalies in the ocean.

Further analyses of the strong intraseasonal variations (~8–9 month time scale) are also necessary.

In the mid-1990s, the equatorial interannual variability is dominated by events, repeating roughly every 17 months, which have the structure of local coupled ocean–atmosphere warm events (zonal wind stress weakening and zonal surface slope relaxation, warm SST, excess precipitation). These Atlantic Niños are modest in amplitude compared to their Pacific counterparts and last for only a few months.

No correlation with ENSO or NAO indices was found. A CWT analysis of SST reveals that frequency of warm events has evolved on decadal time scales during the second part of the 20th century, with a lower frequency in the 1970s and a higher in the 1990s. The periodicity of the Atlantic Niño seems to vary considerably.

Acknowledgments

This research was funded by the French Ministry of Research (ACI Climat), the IRD (Institut de Recherche pour le Développement) and CNES (Centre National de Recherche Spatiale) institutions. We thank Sophie Bouffies-Cloch e for the ERA 40 data, Jonathan Lilly and two anonymous reviewers for their most useful comments.

References

- Arnault, S., Kestenare, E. Tropical Atlantic surface current variability from 10 years of TOPEX/Poseidon altimetry. *Geophys. Res. Lett.* 31 (3), L03308, doi:10.1029/2003GL019210, 2004.
- Carton, J.A., Huang, B. Warm events in the tropical Atlantic. *J. Phys. Oceanogr.* 24, 888–903, 1994.
- Carton, J.A., Cao, X., Giese, B.S., da Silva, A.M. Decadal and interannual SST variability in the tropical Atlantic Ocean. *J. Phys. Oceanogr.* 26, 1165–1175, 1996.
- Chang, P., Saravanan, R., Ji, L., Hegerl, G.C. The effects of local sea surface temperatures on atmospheric circulation over the Tropical Atlantic sector. *J. Clim.* 13, 2195–2216, 2000.

- Handoh, I.C., Bigg, G.R. A self-sustaining climate mode in the tropical Atlantic, 1995–1997: observations and modelling. *Q.J.R. Meteorol. Soc.* 126, 807–821, 2000.
- Jury, M.R., Enfield, D.B., Mélice, J.-L. Tropical monsoons around Africa: stability of El-Niño-Southern Oscillation and links with continental climate. *J. Geophys. Res.* 107, 3151, doi:10.1029/2000JC00507, 2002.
- Katz, E.J., Hisard, P., Verstraete, J.M., Garzoli, S.L. Annual change of sea surface slope along the equator of the Atlantic Ocean in 1983 and 1984. *Nature* 322, 245–247, 1986.
- Okumura, Y., Xie, S.-P. Interaction of the Atlantic equatorial cold tongue and African monsoon. *J. Climate* 17, 3589–3602, 2004.
- Provost, C., Arnault, S., Chouaïb, N., Kartavtseff, A., Bunge, L., Sultan, E. TOPEX/Poseidon and Jason Equatorial Sea Surface Slope Anomaly in the Atlantic in 2002: comparison with Wind and Current Measurements at 23W. *Marine Geodesy* 27, 13769–13774, 2004.
- Ruiz-Barradas, A., Carton, J.A., Nigam, S. Structure of interannual to decadal climate variability in the tropical Atlantic. *J. Climate* 13, 3285–3297, 2000.
- Sutton, R.T., Jrwson, S.P., Rowell, D.P. The elements of climate variability in the tropical Atlantic regions. *J. Climate* 13, 3261–3284, 2000.
- Sverdup, H.U. Wind driven currents in a baroclinic ocean with application to the equatorial currents of the eastern Pacific. *Proc. Natl. Acad. Sci.* 33, 318–326, 1947.
- Tseng, L., Mechoso, C. A quasi-biennial oscillation in the equatorial Atlantic Ocean. *Geophys. Res. Lett.* 28 (1), 187–190, 2001.
- Xie, S.-P., Carton, J.A. Tropical atlantic variability: patterns, mechanisms, and impacts. in: Wang, C., Xie, S.-P., Carton, J.A. (Eds.), *Ocean–atmosphere interactions and climate variability*. AGU Geophysical Monograph, Washington, DC, 2004.
- Zebiak, S.E. Air–sea interactions in the equatorial Atlantic region. *J. Climate* 6, 1567–1586, 1993.